IOSR Journal of Mechanical and Civil Engineering (IOSR-JMCE)
e-ISSN: 2278-1684,p-ISSN: 2320-334X, Volume 16, Issue 2 Ser. IV (Mar. - Apr. 2019), PP 01-12
www.iosrjournals.org

Effect of Hydrochloric Acid on Flexural Behavior of RC Slabs with Calcium Carbonate Nanoparticles

Lamiaa M. Omer[1], Alaa A. El-Sayed[1], Hany A. Dahish[1,] Waleed H. sufe[2]
[1](Civil Engineering, Faculty of Engineering/Fayoum University, Egypt)
[2](Housing and Building National Research Center/ Cairo/ Egypt)
Corresponding Author: Alaa A. El-Sayed

Abstract: *Corrosion is one of the major durability problems that causes serious damage to reinforced concrete slabs in harsh environments. The flexural behavior of concrete slabs subjected to corrosive effects during mixing and/or curing is experimentally investigated in this paper. The harsh environments are simulated by subjecting concrete slabs to different Hydrochloric Acid (HCl) concentrations in deionized water during mixing and/or curing. The effect of adding Calcium Carbonate ($CaCo_3$) as nano-material to mitigate the corrosion problem in concrete slabs is examined. Thirty-one simply supported slabs subjected to corrosive environment are experimentally tested in flexure. One slab is used as reference specimen, while thirty slabs are divided into three groups according to corrosion acceleration periods (one month or three months). In the experimental program, the primary variables are corrosion time, concentrations of the HCl solution in mixing or curing water as well as concentrations of the nanoparticles. Corrosion behavior for the tested slabs is studied by using linear polarization techniques. The flexural behavior of the concrete slabs is investigated by recording the maximum load and deflections at mid-span and at one- third span. Compressive strengths are determined at 28 days and at test day. Based on the experimental program results, it is concluded that significant improvements in the mechanical properties of concrete and high ability to resist aggressive attacks due to adding the ($CaCo_3$) nanoparticles to the concrete mix. Larger compressive strength of cubes is obtained when the HCl concentration is included in mixing water with an increase percentage that reaches 26% compared to the reference slab. The increase in HCl concentration either in mixing or curing water, the larger reduction in the slab peak load as results of deterioration in steel bars. Reduction in bar diameter for the slabs under one-month and three-months accelerated corrosion exposure reached 20% and 49%, respectively.*

Date of Submission: 27-03-2019 Date of acceptance: 11-04-2019

I. Introduction

Corrosion is defined as a chemical or electrochemical reaction between a material and its environment which produces a deterioration of the material properties (Tuutti, 1982). Steel corrosion can cause catastrophic failures in Reinforced Concrete (RC) structures due to the significant loss of strength for the steel bars embedded in concrete in addition to the loss of steel/concrete bond. Corrosion results in the formulation of rust that has a larger volume than the original steel. This rust has poor mechanical properties compared to the original steel properties. Many researchers studied the effect of steel corrosion on the behavior of beams or columns (Mangat and Elgarf, 1999, El-Hefnawi, 2000, Khafaga, 2002, Chung et al., 2008, Darmawan, 2010, Bhargava et al., 2011 and Li et al., 2019). They investigated the reduction in strength of different reinforced concrete element due to the steel corrosion. Chung et al. (2008) carried out an experimental study on RC slabs with corroded and uncorroded reinforcement. The slabs were subjected to a constant current accelerated corrosion technique by applying a direct electric current. The slabs were then tested using four-point bending test to estimate the reduction in their strength due to the reinforcement corrosion. Chung et al. (2008) concluded that a small amount of corrosion increased the load carrying capacity of slabs due to the increase of friction between steel bars and concrete. The increase in the load capacity of slabs reduced when the corrosion level reached about 1% diameter loss. When the diameter loss exceeded 2%, the load carrying capacity of slabs started to decrease. Another experimental study on RC beams was conducted by Darmawan (2010) by using an accelerated corrosion technique. The author estimated the statistical parameters of maximum pit-depths distribution of corroded steel bars in RC beams. A probabilistic analysis was used to combine the pit-depths parameters with the RC beam geometrical and material variables. This was done to determine the effect of corrosion on flexure and shear strengths of RC beams with corroded steel bars. Darmawan (2010) found that pitting corrosion had a less effect on flexure and shear strengths of RC beams than general corrosion. The behavior of RC beams with mild and high-grade corroded steel rebars was investigated by El-Hefnawi (2000).

An accelerated corrosion technique was used by immersing the steel rebars into Calcium Chloride (CaCl) solution for one month. An electric current was then used until the degree of corrosion was reached. El-Hefnawi (2000) concluded that bending stiffness of RC beams with mild or high graded steel slightly increased at low degrees of rebar corrosion. The increase in stiffness was attributed to the bond enhancement resulting from the increase in friction force that developed at the steel-concrete interface. The same study showed that the bending stiffness significantly decreased for RC beams with high degree of rebar corrosion because of the loss of bond. An analytical study on RC beams with corroded reinforcement was conducted by Bhargava et al. (2011). They proposed a set of equations to evaluate time-dependent shear and flexure strengths of corroded RC beams. The study revealed that the shear and flexure strengths of RC beams with corroded reinforcement were linearly correlated to residual cross section and residual bond strength of steel bars. Mangat and Elgarf (1999) observed a significant reduction of flexure strength of beams subjected to corrosion due to the breakdown of bond at the steel/concrete interface. Khafaga (2002) tested a set of RC columns with corroded reinforcement under concentric loading setup. The columns were subjected to an accelerated corrosion technique to reach the required level of corrosion in reinforcing bars. The tests showed that the main factors affecting the residual load carrying capacity of columns subjected to corrosion were concrete cover cracking, spalling, stirrups cutting, bond loss and reduction of corroded rebar cross sections. The tests also showed that significant reduction in the load carrying capacity of columns occurred due to the corrosion of steel rebars.

To mitigate the loss of strength due to corrosion, Kakooei et al. (2012) investigated a method for preventing corrosion of steel and improving the mechanical properties of concrete by adding special materials to RC elements. Polypropylene fibers were used as an additional material in the concrete mix. A set of concrete cylinders reinforced with different ratios and sizes of Polypropylene fibers were tested in a marine environmental condition. Kakooei et al. (2012) found that a volumetric ratio of 1.5 kg/m3 results in a corrosion resistance of steel better than all other samples with different volumetric ratio. Additionally, the experimental program revealed that using Coral aggregate in concrete samples resulted in a corrosion rate of steel twice that of concrete with siliceous aggregate. Sanchez and Sobolev (2010) developed another method to mitigate the loss of strength due to corrosion by using nanotechnology materials. Adding these materials to concrete can lead to the development of sustainable composites with unique mechanical, thermal and electrical properties. A comprehensive survey study on the effect of adding different nano-materials, such as SiO2, Al2O3, Fe2O3, TiO2, CaCO3 and clay, on the behavior of concrete was recently conducted by Reches (2018). One of these materials was the Limestone (i.e. Calcium Carbonate, CaCO3) that was first considered as filler in concrete to partially replace the Ordinary Portland Cement (OPC), as reported by Kakali et al. (2000) and Raki et al. (2010). The addition of nano-CaCO3 to OPC had positive effects on concrete in terms of strength and acceleration of hydration rate (Myers, 2007). However, the efficiency in accelerating the hydration of OPC reduced by the presence of high volumes of supplementary cementitious materials such as fly ash and slag (Sato and Beaudoin, 2007, 2011). Nano-Silica increased the strength, flexibility and durability of concrete, as reported by Garboczi (2009) and Balapour et al. (2018). Moreover, the nano-Silica particles increased the viscosity of the fluid phase of concrete and filled the voids between cement grains. These particles react with Calcium Hydroxide (CaOH) and resulted in more Calcium Silicate Hydrate (CSH) which positively affected the mechanical properties of concrete. Nazari et al. (2010) proposed the usage of Aluminum Oxide (Al2O3) as a partial replacement of cement. They found that the cement could be advantageously replaced with nano-Al2O3 particles up to maximum limit of 2% with an average particle size of 45nm. However, the optimal level of nano-Al2O3 particles content was achieved with 1% replacement because the replacement by nano-Al2O3 decreased workability of fresh concrete. Jung et al. (2018) suggested the usage of Silica Fume (SF) to increase the resistance of reinforced concrete to steel corrosion. They found that SF concrete had lower chloride transport due to the refinement of pore sizes. The same study showed that the reduction of the apparent diffusion coefficient for SF concrete was 74% less than that of OPC concrete and the time to corrosion was 270% higher.

The current paper has three main objectives. The first objective is to experimentally investigate the effect of adding nano-particles to the concrete mix on the flexure behavior of RC slabs. This study adopts the Calcium Carbonate (CaCa3) as a nano-particles material. The second objective is to study the flexural behavior of RC slabs subjected to Hydrochloric Acid (HCl) solution either in mixing water or curing water. The third objective is to evaluate the damage in RC slabs due to the corrosion of the reinforcing steel. This damage is evaluated by estimating the reduction in the peak load of a set of slabs and measuring the reduction in the cross-sectional diameter of steel bars after the corrosion process. The paper starts by discussing the experimental program details including the materials used in the preparation of a set of cubes and RC slabs. This is followed by presenting the details of the adopted corrosion technique and the flexure test setup. Afterwards, the results obtained from the conducted experimental program are presented and discussed.

II. Experimental Investigation

This section shows the properties of the used materials and the procedure of preparing the cubes and RC slabs. Moreover, the details of the Accelerated Corrosion Setup (ACS) that is used to simulate the corrosion process are outlined. Then, the flexure test setup that is utilized to study the flexure behavior of slabs is presented.

i. Materials Properties.

Concrete: Table 1.a shows the chemical composition of the Ordinary Portland Cement (OPC) used in preparing concrete for the tested specimens. An OPC produced by an Egyptian Cement Company is used. The initial and final setting times are 2hr 30min and 5hr 30 min, respectively. The mechanical properties of the gravel and sand are presented in Table 1.b. The concrete mix ingredients for the tested specimens are shown in Table 1.c.

Table 1.a: Chemical composition of OPC.

Chemical component	%
CaO	64.80
SiO2	21.40
Al2O3	6.36
Fe2O3	3.35
MgO	1.85
SO3	1.77
K2O	0.54
Na2O	0.28
TiO2	0.02

Table 1.b. Main physical and mechanical properties for the used gravel and sand.

Gravel	
Unit Weight	1.60 t/m^3
Specific Gravity	2.86
Crushing Coefficient	13.76%
Sand	
Unit Weight	1.67 t/m^3
Specific Gravity	2.5

Table 1.c. Concrete mix ingredients and amounts.

Material	Amount
Cement	350 kg/m^3
Basalt	1291 kg/m^3
Sand	633 kg/m^3
Water	175 liters

Steel reinforcement

For the tested slabs, high grade deformed steel bars with a diameter of 10 mm and mild steel plain bars with a diameter of 8 mm are used as main and secondary reinforcement, respectively. Table 2 shows the geometric and mechanical properties for both the high grade and mild steel bars.

Table (2): Geometric and mechanical properties of reinforcement bars.

Type of steel	Nominal bar diameter (mm)	Actual bar diameter (mm)	Actual cross sectional area (mm^2)	Yield stress (N/mm^2)	Ultimate strength (N/mm^2)	Elongation (%)
High grade	10	10.5	86	445.6	611.1	10
Mild	8	7.7	47	303.3	460.2	25

ii Preparation of specimens

Thirty-one reinforced concrete slabs with plan dimensions of 1200x500 mm and a thickness of 80 mm are prepared. The diameter of the main and secondary reinforcement is 10 mm and 8 mm, respectively. One slab is used as reference specimen, fifteen slabs are treated by nano particles (CaCo3) and the other fifteen slabs are not treated. The thirty slabs are divided into three groups (Group 1: without accelerated corrosion system, Group 2: with accelerated corrosion system for one month, and Group 3: with accelerated corrosion system for two months). Each slab is denoted by an identification name that represents the conditions at which the slab is casted and cured. The letter "B" in the slab name indicates that the specimen is immersed in the HCl solution while the letter "A" indicates that the specimen is not immersed in the HCl solution. The letter "U" indicates that no nano-

material is used in preparing the specimen while the letter "N" indicates that CaCo3 particles are used in preparing the specimen.

The reinforcement mesh for each slab is placed in wooden forms and then concrete mix is casted. The steel reinforcement arrangement is shown in Fig. 1 where high-grade and mild steel bars are placed in the main and secondary directions, respectively. Concrete mix was designed to produce concrete with a compressive strength of 25 N/mm2. The concrete was mixed in a rotating mixer of 100 liters capacity and was then compacted using an electrical poker vibrator. Figs. 2.a, 2.b and 2.c show the stages of casting of the concrete mix into the wooden forms. Curing of the RC slabs was twice a day for a week by using burlap, as shown in Fig. 2.d. The slabs are stored in the laboratory till the end of the accelerated corrosion exposure. During casting of the specimens, four standard cubes with an edge length of 150 mm are taken, compacted by electrical vibrator and cured for a week according to the Egyptian Manual of Laboratory Tests for Concrete Materials (2003). The cubes are tested after 28 days and the average compressive strength are recorded in Table 3.

Figure (1). Steel reinforcement arrangement in wooden form.

Figure (2). a. Preparing of the concrete mix ingredients.

Figure (2). **b.** Mixing of concrete.

Figure (2). c. Compacting of concrete.

Figure (2). d. Curing of slabs.

Table (3) Compressive and tensile strengths for the samples after 28 days.

Slab Indent	SAU01 SAU02 SAU03	SAN01 SAN02 SAN03	SAN21 SAN22 SAN23	SAN51 SAN52 SAN53	SAU21 SAU22 SAU23	SAU51 SAU52 SAU53	SBU21 SBU22 SBU23	SBU51 SBU52 SBU53	SBN21 SBN22 SBN23	SBN51 SBN52 SBN53
Compressive strength (N/mm^2)	41.57	45.32	38.19	44.84	42.44	40.95	41.41	41.51	35.29	38.70
Tensile strength (N/mm^2)	4.69	5.20	4.13	4.80	4.72	4.33	4.61	4.62	3.82	4.03

iii Accelerated corrosion setup (ACS)

In the current study, an accelerated corrosion technique is adopted to induce the corrosion process in a relatively short time in laboratory environment compared to the long period occurring in real life environment. A schematic and a photo for the three slabs subjected to the adopted corrosion technique are presented in Fig. 3. Ten tanks are filled with Hydrochloric Acid (HCl) solution, which worked as electrolyte, with concentration of 0%, 2% and 5%. Stainless steel bars are placed into the tanks and work as cathode while the reinforcing steel bars in the slabs act as anode. Three slabs are placed in each tank. A Direct Current (DC) power supply with variable resistance is used to cause a rate of $1mA/cm^2$. The specimens are immersed in the HCl solution for three weeks before applying the DC. The setup is applied for two different periods (one month and three months). Table 4 illustrates the nano-material concentrations, the HCl solution aggression percentages and the exposure to corrosion periods for the tested RC slabs. The electrochemical measurements are determined by Voltalab 10 PGZ100 "all- in -one" Potentiostate / Galvanostate system performed in temperature 21ºC and humidity of 45%.

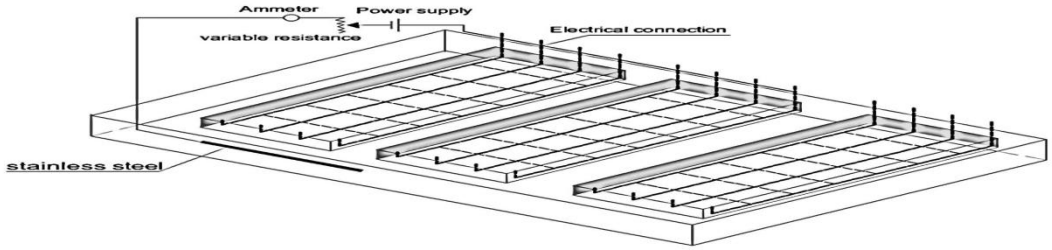

Figure (3). Adopted ACS (a) schematic for three slabs

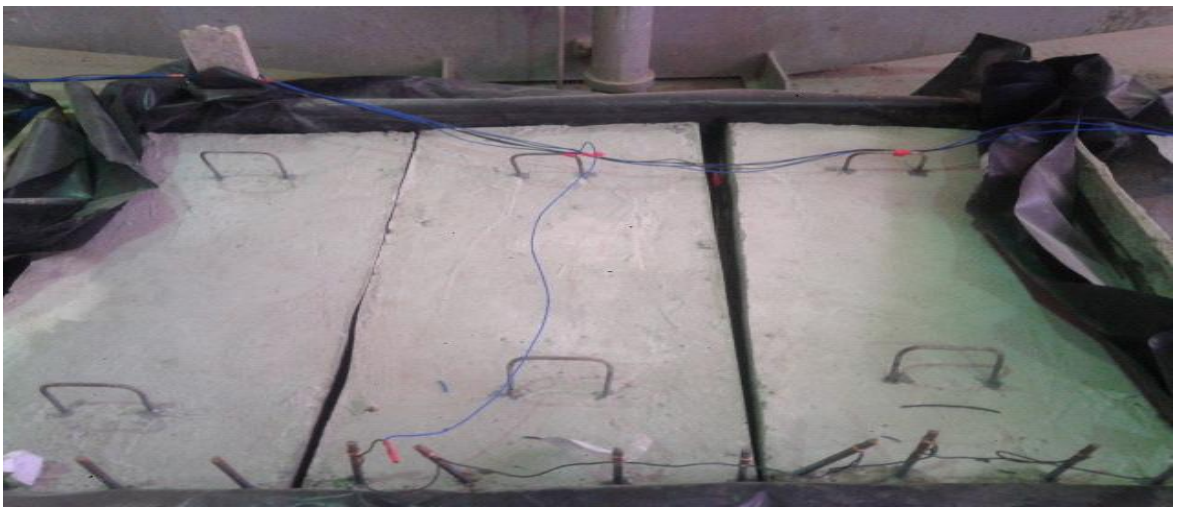

Figure (3). Adopted ACS (b) photo for three slabs from the lab.

Table (4). Nano material concentration, HCl aggression and corrosion exposure for tested slabs.

Slabs Indent.	Nano concentration	HCl solution aggression	Exposed to corrosion period (month)
S1	---	---	---
SAU01	---	---	---
SAU02	---	---	1
SAU03	---	---	3
SAN01	5% of mixing water	---	---
SAN02	5% of mixing water	---	1
SAN03	5% of mixing water	---	3
SAU21	---	2% in mixing water	---
SAU22	---	2% in mixing water	1
SAU23	---	2% in mixing water	3
SAN21	5% of mixing water	2% in mixing water	---
SAN22	5% of mixing water	2% in mixing water	1
SAN23	5% of mixing water	2% in mixing water	3
SAU51	---	5% in mixing water	---
SAU52	---	5% in mixing water	1
SAU53	---	5% in mixing water	3
SAN51	5% of mixing water	5% in mixing water	---
SAN52	5% of mixing water	5% in mixing water	1
SAN53	5% of mixing water	5% in mixing water	3
SBU21	---	Immersed in 2% HCl sol.	---
SBU22	---	Immersed in 2% HCl sol.	1
SBU23	---	Immersed in 2% HCl sol.	3
SBN21	5% of mixing water	Immersed in 2% HCl sol.	---
SBN22	5% of mixing water	Immersed in 2% HCl sol.	1
SBN23	5% of mixing water	Immersed in 2% HCl sol.	3
SBU51	---	Immersed in 5% HCl sol.	---
SBU52	---	Immersed in 5% HCl sol.	1
SBU53	---	Immersed in 5% HCl sol.	3
SBN51	5% of mixing water	Immersed in 5% HCl sol.	---
SBN52	5% of mixing water	Immersed in 5% HCl sol.	1
SBN53	5% of mixing water	Immersed in 5% HCl sol.	3

v. Flexure test setup

As shown in Fig. 4, the RC slabs are subjected to six concentrated loads in a flexural test to investigate their behavior. A reaction frame is used in the test with a capacity of 100 tons and a stroke of 300 mm. A set of Linear Variable Displacement Transducers (LVDT) with a stroke of 100 mm and a sensitivity of 0.1 mm are used in the horizontal and vertical directions. The vertical LVDTs are placed in middle and one-third of the slab span to measure the deflection in the vertical direction. The horizontal LVDTs are placed in the middle of the span to measure the strain in the horizontal direction. The arrangement and locations of the LVDTs and supports are shown in Fig. 4. After conducting the flexure test for each slab, the rebars are extracted from the slabs and then are cleaned from the corrosion production. Then, the cross-sectional diameters are measured using Vernier Caliper for each slab in three different positions along the slab length side. The average cross-sectional diameter for the rebars of each slab is recorded.

Figure (4). Schematic of flexure test setup.

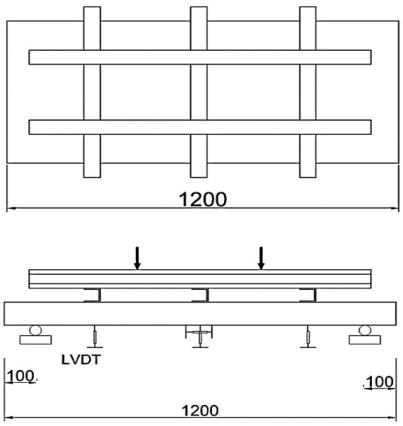

Figure (5) . Schematic of supports and LVDTs locations.

III. Results and Discussion

The results obtained from the flexure test of the thirty-one RC slabs under vertical loads are plotted and discussed in this section. Comparisons between the results of the following behavioral aspects for the tested slabs are investigated: load–deflection relation, compressive strength of standard cubes, and the reduction in the reinforcing bar cross sections due to corrosion. The results of all slabs are compared to those of the reference slab, S1.

Load- deflection relationships

Fig. 6 shows the load-deflection relation for all the tested RC slabs where the deflection is measured at the mid-span. The load-deflection relation for the reference slab S1 is compared to those of the slabs SAU01, SAU21, SAU51 with ratios of HCl in mixing water of 0%, 2% and 5%, respectively, as shown in Fig. 6a. The figure illustrates the effect of changing the HCl concentration in mixing water or in curing water on peak load and displacements. The peak load of slabs SAU01, SAU21 and SAU51 is larger than that of reference slab S1 by 119%, 115% and 106%, respectively because the compressive strength of these slabs is larger than that of refence slab by 14%. The deflection at failure for slabs SAU01 and SAU 21 is less than that of the reference slab while the deflection at failure for slab SAU 51 is larger than that of the reference slab. This indicates that increasing the HCl in mixing water results in more ductile behavior for RC slabs. Additionally, one can notice that increasing the HCl amount in mixing water reduces the peak load of the RC slabs. This reduction reaches 11% corresponding to a percentage of 5% of HCl in mixing water. Fig. 5a also shows the load-midspan deflection relation for slabs SBU21 and SBU51 where the RC slabs are immersed in HCl solution during curing with an amount of 2% and 5% of curing water, respectively. One can observe that adding HCl in curing water reduces the deflection at peak load by percentage that reached 26% corresponding to an amount of 2% of HCl in curing water.

Fig. 5b shows the effect of changing the HCl concentration in mixing water or in curing water on peak load and displacement of the RC slabs with 5% nano-$CaCo_3$ particles added in mixing water. The peak load of slab SAN01 is smaller than that of the reference slab S1 by 16% while the peak load of both slabs SAN21 and SAN51 is larger than that of the reference slab S1 by 120%. This indicates that adding nano-particles without having HCl in the mixing water of RC slabs reduces the peak load of the RC slabs. However, the opposite trend is noticed when both nano-particles and HCl solution are added to mixing water of the RC slabs. Fig. 6b also shows the effect of adding 5% of nano-particles to the mixing water and immersing the RC slab into different amount of HCl during curing. Comparing the peak load for RC slabs SBN51 to slab SBN 21, which have same amount of the nano-$CaCo_3$ of 5%, a reduction of 20% occurred when the amount of HCl solution increased in curing water from 2% to 5%. Fig. 6c and 6d depict the effect of applying ACS for one month on the peak load and deflection at peak load of RC slabs. The behavior of the tested slabs is studied without nano-particles in Fig. 6c where the load-midspan relation of slabs SAU02, SAU22, SAU52, SBU22 and SBU 52 is plotted.

The load-deflection relation for the reference slab S1 is compared to those of the RC slabs SAU02, SAU22, SAU52 without nano-particles and with ratios of HCl in mixing water of 0%, 2% and 5%, respectively, as shown in Fig. 6c. The same figure also shows the load-deflection relation of slabs SBU22 and SBU52 with HCl concentration in curing water of 2% and 5%, respectively. All the aforementioned slabs are subjected to a one-month ACS. The effect of changing the HCl concentration in mixing water or in curing water on peak load and displacements of the RC slabs can be withdrawn from Fig. 6c. The peak load of slab SAU02 is larger than that of reference slab S1 by 110% because the compressive strength of slab SAU02 is larger than that of refence slab by 14%. However, the peak load of slabs SAU22 and SAU52 is less than that of reference slab S1 by 14% and 24%, respectively. This reduction in the peak load occurred due to having HCl aggression in mixing water which has a negative effect on the RC slab capacity. The midspan deflection at failure for slab SAU52 is less than that of slab SAU22 and the midspan deflection at failure for slab SAU22 is less than that of slab SAU02. This indicates that increasing the HCl aggression in the mixing water results in less ductile behavior for RC slabs in case of a one month ACS. Moreover, it can be noted that increasing the HCl amount in mixing water reduces the peak load of the RC slabs which are subjected to a one-month ACS. Referring to the load-midspan deflection relation for slabs SBU21 and SBU51 in Fig. 6c, one can observe that adding the HCl solution in curing water reduces the deflection at peak load by a percentage of 33% and 40% corresponding to an amount of 2% and 5% of HCl solution in curing water.

Fig. 6d shows the effect of changing the HCl concentration in mixing water or in curing water on peak load and displacement of the RC slabs with 5% nano-$CaCo_3$ particles added in mixing water and subjected to a one-month ACS. The peak load of slab SAN22 is larger than that of the reference slab S1 by 10% while the peak load of both slabs SAN02 and SAN52 is less than that of the reference slab S1 by 5% and 25%, respectively. This indicates that, for the slabs with 5% nano-particles, adding HCl in the mixing water of RC slabs can change the peak load of the RC slabs by a percentage that reaches to 25%. However, it is clear from

Fig. 6d that a significant reduction in the peak load occurs when the HCl percentage in curing water increases from 2% to 5% in slabs SBN22 and SBN52, respectively.

Also, one can notice the deflection at failure of slab SBN52 is significantly less than that of slab SBN22 due to increasing the HCl in curing water from 2% to 5%.

The effect of adding nano-particles on the behavior of RC slabs, which are subjected to three-month ACS, can be withdrawn from Figs. 6e and 6f. The same figures also show the effect of changing the HCl concentration either in mixing water or curing water for a set of slabs. One can observe that a significant reduction in both the peak load and mid-span deflection at failure for all slabs compared to the reference slab S1. The reduction in the peak load ranges between 49% and 62% while the reduction in the mid-span deflection at failure ranges between 49% and 68%. These reductions occur due to subjecting the specimens to a three-month period of accelerated corrosion exposure. Fig. 6e shows the load deflection relation for the reference slab S1 along with slabs SAU03, SAU23 and SAU53 where HCl solution is applied on mixing water with a percentage of 0%, 2% and 5%, respectively. It is observed that the peak load and mid-span deflection at failure increase when the HCl in mixing water percentage increased from 0% to 5%. The same figure also shows the load-deflection relation for slabs SBU23 and SBU53 where the specimens are subjected to 5% of HCl in curing water. One can note that the peak load and deflection at failure increase by percentages of 8% and 9%, respectively, when the amount of HCl in curing water increases from 2% to 5%. Comparing the behavior of slabs SAU03 with SAN03, one can observe that no change occurs in the peak load while the mid-span deflection at failure increases by 67%. This indicates that adding nano-particles to the RC slabs increases the ductility significantly and has slight effect on the capacity of the RC slabs. Same conclusions can be found by comparing the behavior of slabs SAU53 and SAN53 with slight reduction in the peak load and increase in the mid-span deflection by 34%. Reduction in the mid-span peak load and deflection at failure can be observed by 19% and 16%, respectively, when the load deflection of slab SBU 23 in Fig. 6e is compared with that of SBN23 in Fig. 6f. This means that adding nano-particles to the RC slabs has a negative effect on both the capacity and ductility. However, the peak load increases by 32% and the mid-pan deflection at failure decreases by 11% when the load deflection curve of slab SBU53 is compared to that of SBN53.

Referring to Fig. 6, it can be noticed that the largest reduction in peak load occurs in slab SBN23, where 5% of mixing water nano-particles is used and the slab is immersed into HCl exposure of 2% and subjected to three-month ACS. The largest reduction in mid-span deflection at failure occurs in slab SAU03, no nano-particles is used and the slab is under three-month ACS and is not subjected to HCl during mixing or curing. One can observe that slabs which are exposed to ACS for three months have the largest reduction in peak load. The reduction in the peak load for the three-month exposed RC slabs reaches 69% compared to the reference slab peak load. The reduction in the peak load of the RC slabs which were exposed to ACS for one month reaches 30% compared to the reference slab peak load. Similar conclusions can be withdrawn from the load- deflection relationships at one-third span for the tested RC slabs which are plotted in Figure. 7.

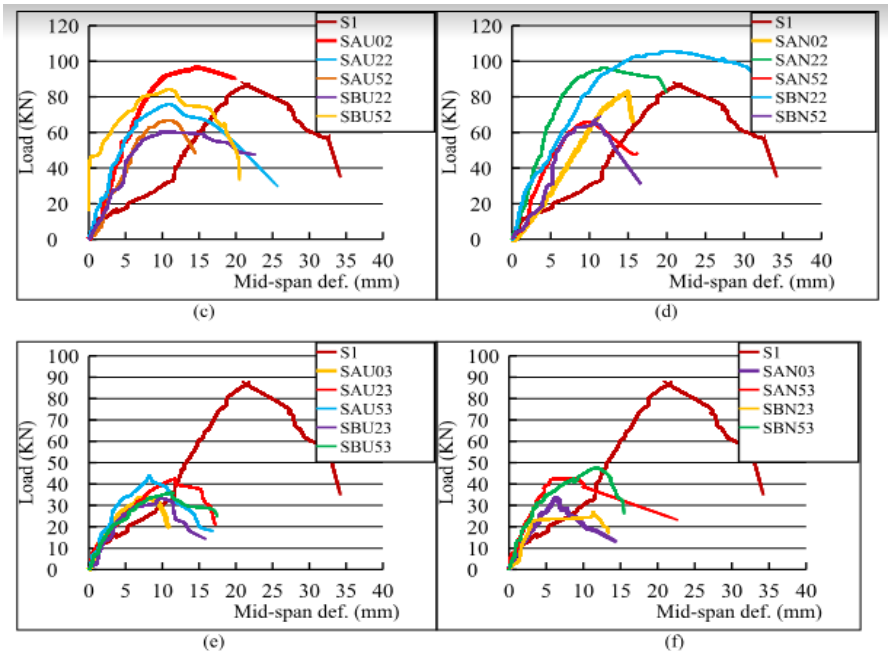

Figure (6). Load-midspan deflection for tested slabs (a) without ACS without nano-particles (b) without ACS with nano-particles (c) with one month ACS without nano-particles (d) with one month ACS with nano-particles (e) with three months ACS without nano-particles (f) with three months ACS with nano-particles.

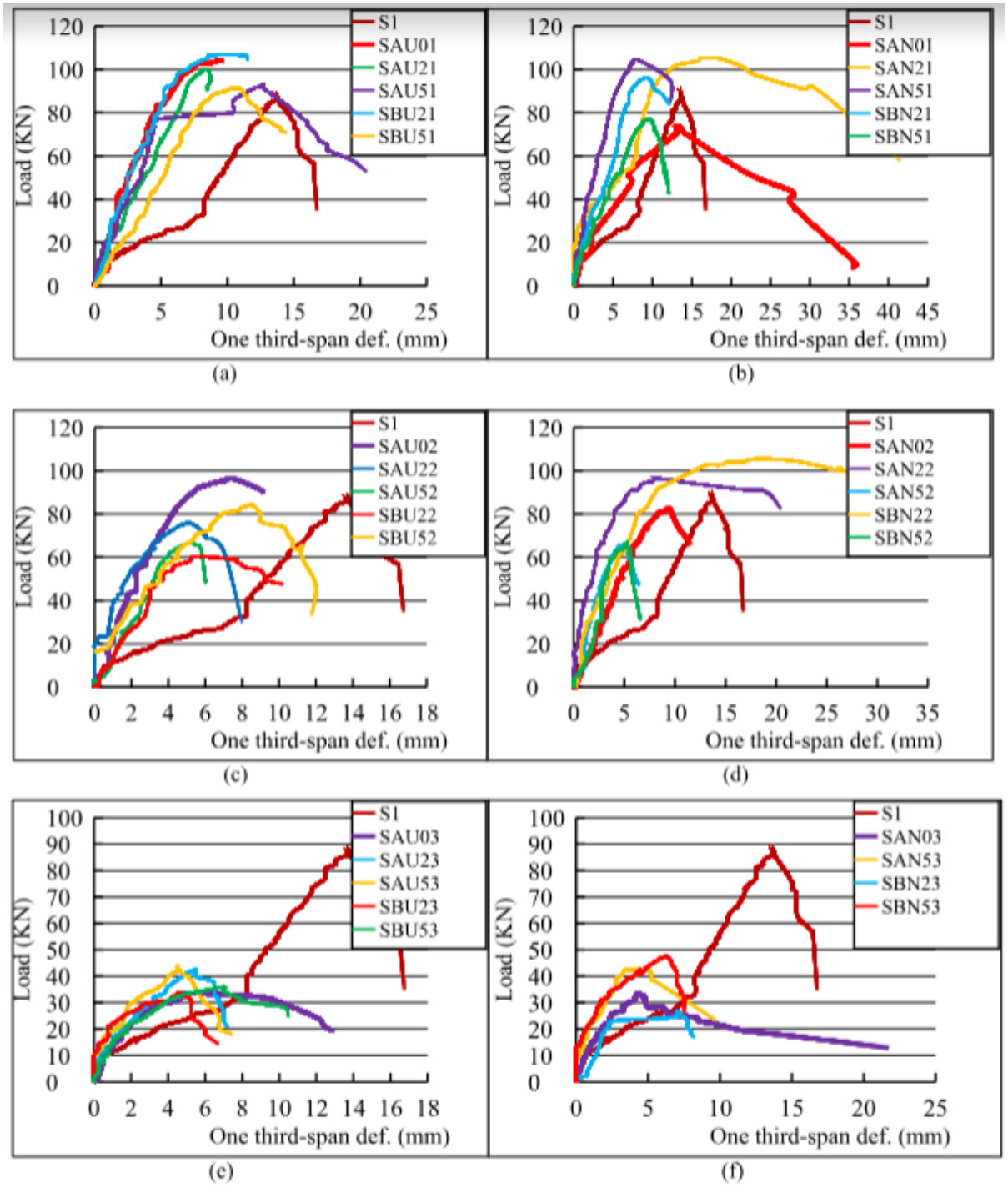

Figure (7). Load-one third span deflection for tested slabs (a) without ACS without nano-particles (b) without ACS with nano-particles (c) with one-month ACS without nano-particles (d) with one month ACS with nano-particles (e) with three months ACS without nano-particles (f) with three months ACS with nano-particles.

Compressive strength

Fig. 8 shows the effect of different parameters (adding HCl to mixing or curing water, adding nano-material and exposure to accelerated corrosion) on compressive strength of the standard cubes which are taken from the concrete mix of the tested RC slabs. The f_{cu} of the slabs SAU0 is larger than that of the reference slab S1 due to conducting the compression test after 28 and 60 days for the reference slab and slabs SAU0, respectively. An increase of 25% in the f_{cu} for slabs SAN0 more than SAU0 is observed due to adding nano-material in the mixing water**.** Fig. 8 shows that insignificant difference is noted between the f_{cu} of slabs SAU0 and SAU2, which includes 2% HCl in mixing water. This indicates that the existence of the HCl solution in

mixing water accelerates the hydration in concrete and therefore increases the compressive strength. The ratio of f_{cu} for SAN0 to SAU0, SAN2 to SAU2 and SAN5 to SAU5 is 1.3, 1.1 and 1.1, respectively, which shows that adding nano-material to RC slabs increases the compressive strength when they are subjected to 0%, 2% and 5% of HCl solution in mixing water. One can observe that the ratio of f_{cu} for both SBN2 to SBU2 and SBN5 to SBU5 is 1.04, which illustrates a slight increase in the compressive strength when a nano-material is added to the cubes immersed in HCl during curing. Fig. 8 shows that insignificant difference in f_{cu} exists for the cubes of the slabs SAU0, SAU2 and SAU5, which implements that adding HCl solution in mixing water does not affect the compressive strength of the cubes. However, the existence of HCl solution in curing water causes damage in concrete and therefore reduces the compressive strength. This can be noticed when the f_{cu} for the slabs SBU2 and SBU5 is compared to that of slabs SAU0. The reduction in the f_{cu} reaches 22% when the cubes are immersed in 5% of HCl solution in curing water.

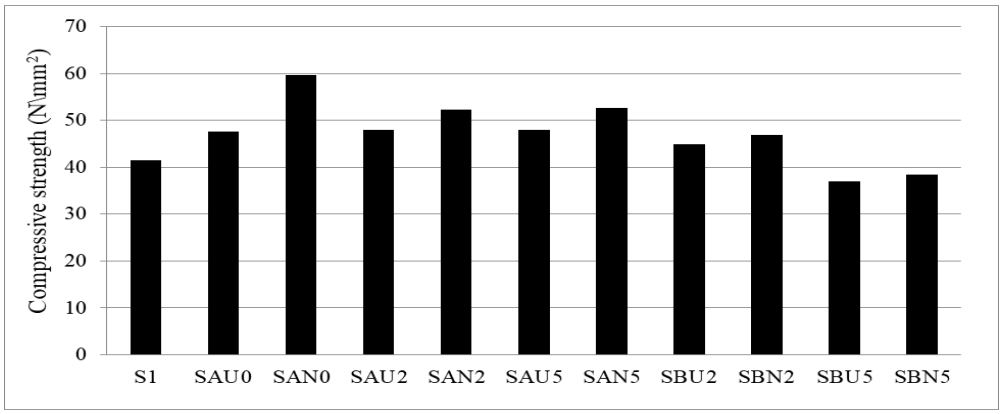

Figure (8). Compressive strength for the tested RC slabs.

Reduction in rebar diameters

The bar diameter for all the tested RC slabs after conducting the flexure test is plotted in Fig. 9. It can be concluded that adding HCl solution has a significant effect on reducing the rebar cross-sectional diameter. One can observe that adding the HCl solution in mixing water decreases the rebar cross-sectional diameter more than the reduction due to the existence of HCl solution in curing water. Fig. 9 shows that slab SAN53, without nano-material and with 5% of HCl in mixing water and subjected to three-month ACS, have the most reduction in rebars cross-sectional diameter. The maximum bar diameter is noted to be in slab SAN51, with 5% nano-material and with 5% of HCl in curing water, which is not subjected to acceleration corrosion exposure. Photo of one reinforcing steel bar for slabs SAN53 and SAN51 after conducting the test is presented in Fig. 10. It is clear from Fig. 9 that exposing the slabs to one-month ACS reduces the bar diameter with a percentage that ranges between 3% and 20%. Also, exposing the slabs to three-month ACS reduces the bar diameter with a percentage that ranges between 5% and 49%.

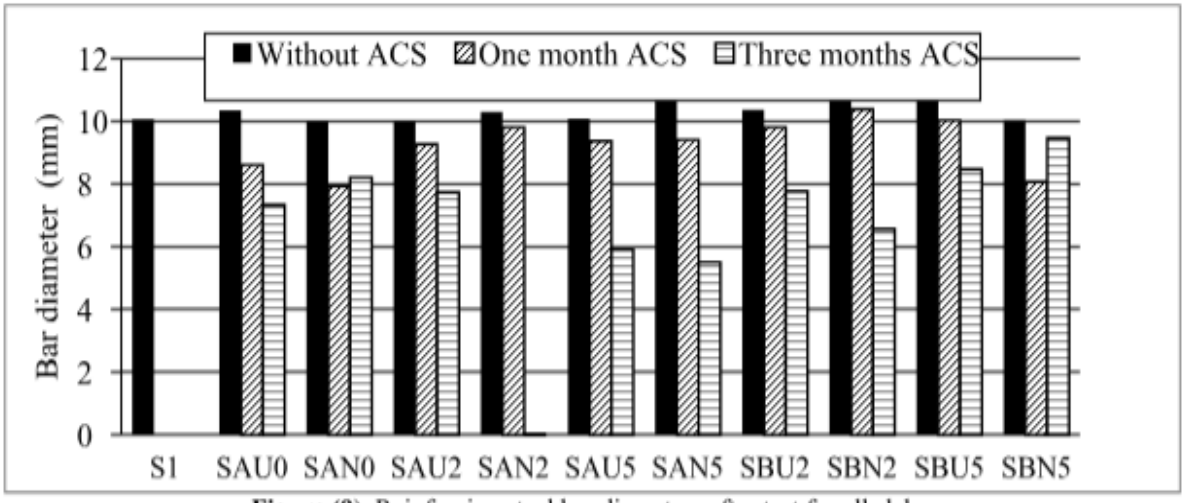

Figure (9). Reinforcing steel bar diameters after test for all slabs.

Figure (9). Photos for reinforcing steel bar after conducting the flexure test for slabs SAN51 and SAN53.

IV. Conclusion

Thirty-one Reinforced Concrete (RC) slabs, treated by nano-material and exposed to aggressive solution, were tested into an Accelerated Corrosion Setup (ACS) to study their behavior in aggressive environments. The Calcium Carbonate (CaCo3) and Hydrochloric Acid (HCl) were adopted as nano-material and aggressive solution, respectively. The reinforcing steel bars in the slabs worked as anode, stainless-steel plate acted as cathode, as well as the HCl solution worked as electrolyte in the ACS. A Direct Current (DC) power supply and a variable resistance were utilized. One slab was used as reference specimen, while the rest thirty slabs were divided into three groups (without accelerated corrosion system, with accelerated corrosion system for one month and with accelerated corrosion system for three month). The slabs were subjected to different HCl concentrations (0%, 2% and 5%) in mixing and/or curing water. Compression tests were conducted for cubes subjected to same environmental conditions of the slabs to obtain the compressive strength for each slab. The thirty-one slabs were tested under flexure and the load-deflection relation was recorded at both mid-span and one-third span points. The rebars were then extracted from the slabs and the cross-sectional diameters were measured using Vernier Caliper. Based on the conducted tests, the following conclusions can be drawn:

- Reduction in the slab peak load increased for longer period of ACS due to the deterioration of the steel rebars.
- Reduction in the peak load for the three-month and one-month exposed RC slabs reached 69% and 30%, respectively, compared to the reference slab peak load.
- Largest reduction in peak load occurred in a slab with 5% of mixing water nano-material, immersed into HCl exposure of 2% and subjected to three-month ACS.
- Largest reduction in mid-span deflection at failure than that of reference slab occurred in a slab without nano-particles, subjected to three-month ACS and was not subjected to HCl during mixing or curing.
- Reduction in compressive strength of the RC slabs which were exposed to aggressive medium in curing water was higher than that of RC slabs with aggressive medium in mixing water.
- Compressive strength of slabs with 2% and 5% HCl concentration in mixing water was higher than that of slabs without any aggressive medium as result of the increase in hydration rate in the presence of HCl in mixing water.
- The bar diameter after the flexure test for the slabs with nano-material and subjected to aggressive medium was larger than that of slabs without nano-material due to the effect of adding CaCo3 to mixing water which caused contention interstitial on steel bars and increased the bar size.
- The increase in HCl concentration in slabs either in mixing or curing water, the larger reduction in ultimate load capacity as a result of deterioration in steel bars.

- The percentage range of reduction in bar diameter for the slabs under one-month and three-months ACS was 3~20% and 5~49%, respectively.
- Random failures were observed in the tested slabs due to the increase in permeability in localized parts of the slabs. Accordingly, it is recommended using graded aggregates with small sizes and fully compaction for concrete during casting to reduce the deterioration of concrete in aggressive environments.

References

[1]. Balapour, M., Joshaghani, A. and Althoey, F., 2018. Nano-SiO2 contribution to mechanical, durability, fresh and microstructural characteristics of concrete: A review. Construction and Building Materials, 181, pp.27-41.

[2]. Bhargava, K., Mori, Y. and Ghosh, A.K., 2011. Time-dependent reliability of corrosion-affected RC beams—Part 1: Estimation of time-dependent strengths and associated variability. Nuclear Engineering and Design, 241(5), pp.1371-1384.

[3]. Chung, L., Najm, H. and Balaguru, P., 2008. Flexural behavior of concrete slabs with corroded bars. Cement and Concrete Composites, 30(3), pp.184-193.

[4]. Darmawan, M.S., 2010. Pitting corrosion model for reinforced concrete structures in a chloride environment. Magazine of Concrete Research, 62(2), pp.91-101.

[5]. Egyptian Concrete Committee. 2003. The Egyptian Manual for Laboratory Tests of Concrete Materials-The Egyptian Code for Design and Construction of Concrete Structures. ECP Committee 203-2003.

[6]. El-Hefnawi, A. A., 2000. A New Statistical Approach For Predicting The Residual Capacity Of Reinforced Concrete Beams Having Corroded Main Steel. Ph.D. Thesis, Faculty of Engineering, Cairo University, Egypt.

[7]. Garboczi, E.J., 2009. Concrete nanoscience and nanotechnology: Definitions and applications. In Nanotechnology in Construction 3 (pp. 81-88). Springer, Berlin, Heidelberg.

[8]. Jung, M. S., Kim, K. B., Lee, S. A., & Ann, K. Y., 2018. Risk of chloride-induced corrosion of steel in SF concrete exposed to a chloride-bearing environment. Construction and Building Materials, 166, pp.413-422.

[9]. Kakali, G., Tsivilis, S., Aggeli, E. and Bati, M., 2000. Hydration products of C3A, C3S and Portland cement in the presence of CaCO3. Cement and Concrete Research, 30(7), pp.1073-1077.

[10]. Kakooei, S., Akil, H.M., Dolati, A. and Rouhi, J., 2012. The corrosion investigation of rebar embedded in the fibers reinforced concrete. Construction and Building Materials, 35, pp.564-570.

[11]. Khafaga, M. A., 2002. Experimental And Theoretical Study For Estimating The Structural Behavior And The Residual Capacity Of Reinforced Concrete Short Columns With Corroded Rebars. Ph.D. Thesis, Faculty of Engineering, Cairo University, Egypt.

[12]. Li, Z., Jin, Z., Zhao, T., Wang, P., Li, Z., Xiong, C., and Zhang, K., 2019. Use of a novel electro-magnetic apparatus to monitor corrosion of reinforced bar in concrete. Sensors and Actuators A: Physical, 286, pp.14-27.

[13]. Mangat, P.S. and Elgarf, M.S., 1999. Flexural strength of concrete beams with corroding reinforcement. Structural Journal, 96(1), pp.149-158.

[14]. Myers R, Calcium carbonate. 2007. In 100 Most Important Chemical Compounds: A Reference Guide. Greenwood Press, Westport, CT, USA, pp. 59–61.

[15]. Nazari, A., Riahi, S., Riahi, S., Shamekhi, S.F. and Khademno, A., 2010. Influence of Al2O3 nanoparticles on the compressive strength and workability of blended concrete. Journal of American Science, 6(5), pp.6-9.

[16]. Raki, L., Beaudoin, J., Alizadeh, R., Makar, J. and Sato, T., 2010. Cement and concrete nanoscience and nanotechnology. Materials, 3(2), pp.918-942.

[17]. Reches, Y., 2018. Nanoparticles as concrete additives: Review and perspectives. Construction and Building Materials, 175, pp.483-495.

[18]. Sanchez, F. and Sobolev, K., 2010. Nanotechnology in concrete–a review. Construction and building materials, 24(11), pp.2060-2071.

[19]. Sato, T. and Beaudoin, J.J., 2007. The Effect of nano-sized CaCO3 addition on the hydration of cement paste containing high volumes of fly ash. In Proceedings of the 12th International Congress on the Chemistry of Cement (pp. 8-13). Montreal, Quebec, Canada.

[20]. Sato, T. and Beaudoin, J.J., 2011. Effect of nano-CaCO3 on hydration of cement containing supplementary cementitious materials. Advances in Cement Research, 23(1), pp.33-43.

[21]. Tuutti, K., Corrosion of Steel in Concrete, 1982. Swedish Cement and Concrete Research Institute, Stockholm, Sweden.

Lamiaa M. Omer. “Effect of Hydrochloric Acid on Flexural Behavior of RC Slabs with Calcium Carbonate Nanoparticles .” IOSR Journal of Mechanical and Civil Engineering (IOSR-JMCE) , vol. 16, no. 2, 2019, pp. 01-12